Minimizing Pulling Geometry Errors in Atomic Force Microscope Single Molecule Force Spectroscopy

Monica Rivera,* Whasil Lee,* Changhong Ke,† Piotr E. Marszalek,* Daniel G. Cole,‡ and Robert L. Clark*
*Department of Mechanical Engineering and Materials Science, Center for Biologically Inspired Materials and Materials Systems, Pratt School of Engineering, Duke University, Durham, North Carolina 27708; †Department of Mechanical Engineering, State University of New York at Binghamton, Binghamton, New York 13902; and ‡Department of Mechanical Engineering and Materials Science, University of Pittsburgh, Pittsburgh, Pennsylvania 15261

ABSTRACT In atomic force microscopy-based single molecule force spectroscopy (AFM-SMFS), it is assumed that the pulling angle is negligible and that the force applied to the molecule is equivalent to the force measured by the instrument. Recent studies, however, have indicated that the pulling geometry errors can drastically alter the measured force-extension relationship of molecules. Here we describe a software-based alignment method that repositions the cantilever such that it is located directly above the molecule's substrate attachment site. By aligning the applied force with the measurement axis, the molecule is no longer undergoing combined loading, and the full force can be measured by the cantilever. Simulations and experimental results verify the ability of the alignment program to minimize pulling geometry errors in AFM-SMFS studies.

INTRODUCTION

Since its conception by Binnig, Quate, and Gerber in 1986 (1), the atomic force microscope (AFM) has become a powerful tool to study the properties of single molecules (2–4). In AFM-based single molecule force spectroscopy (AFM-SMFS), molecules are stretched by increasing the distance between the substrate and the cantilever to which the molecule is attached. By measuring the vertical deflection of the microcantilever throughout the pulling process, one is able to ascertain the forces required to stretch the molecule. The resulting force-extension profile can then be used to gain insight into the secondary and tertiary structure of the molecule.

A key assumption in AFM-SMFS experiments is that the pulling angle is negligible and the measured forces and extensions are equivalent to the actual values experienced by the molecule. This assumption however, may be incorrect (5–7). Depending on the structure of the molecule and/or the manner in which the molecule is attached to the surface, it is possible for the cantilever and substrate attachment sites to be separated by significant distances in the x, y plane, such as that seen in Fig. 1 *A*. In such a case, movement of the AFM's piezoelectric z stage will cause the molecule to experience combined loading, or loading in more than one direction (assuming that the molecule is stretched in the z direction). Because the force on the molecule is measured indirectly through the use of a microcantilever, only the z component of the total force acting on the molecule is recorded by the AFM, leading to an underestimation of encountered forces. The measured extension of a molecule is also subject to pulling geometry effects in that only the vertical cantilever-substrate separation distance is recorded.

To illustrate the effects of lateral offsets on AFM-SMFS measurements, a basic study investigating the effects of lateral separation distances on the measured extension and pulling velocity was conducted. In this study, a rigid structure with an original length of 100 nm was attached to the origin of a theoretical sample surface. Using simple geometric principles, the length (L) of the rigid molecule was systematically increased to 200 nm at a velocity (dL/dt) of 1 nm/s. A plot of the measured (Z) versus actual (L) molecule lengths for various lateral separation distances can be found in Fig. 1 *B*. As anticipated, the measured length of the molecule is less than the actual length of the molecule, with errors increasing with increasing lateral offset distances. Furthermore, because the angle (α) of the molecule changes throughout the pulling process, the extension errors vary as the molecule is extended, with errors decreasing with increasing extension.

Pulling geometry effects can also impact the pulling velocity and loading rates experienced by the molecule. Because these stretching methods are regulated by the z stage retraction speed and the vertical deflection of the cantilever, respectively, unsteady stretching of the molecule can occur. For instance, Fig. 1 *C* shows the actual pulling velocity experienced by the rigid molecule (dL/dt) for a vertical or z stage retraction rate (dZ/dt) of 1 nm/s. For a perfectly aligned molecule (*solid line*), the velocity is constant throughout the pulling cycle. However, as the lateral separation distance increases, the actual pulling velocity (dL/dt) decreases, with velocity errors approaching 85%. As with the extension errors, due to changes in the angle of the molecule, the velocity errors are not constant throughout the pulling process. Pulling rates would also be subject to errors in that only the z component of the force is measured throughout the pulling cycle. Because single molecule behavior is highly dependent upon the loading rate (8,9),

Submitted May 29, 2008, and accepted for publication June 26, 2008.

Address reprint requests to Dr. Robert L. Clark, Dept. of Mechanical Engineering and Materials Science, Duke University, Box 90300, Durham, NC 27708. Tel.: 919-660-5435; Fax: 919-660-5409; E-mail: rclark@duke.edu.

Editor: Jane Clarke.

0006-3495/08/10/3991/08 $2.00

doi: 10.1529/biophysj.108.138842

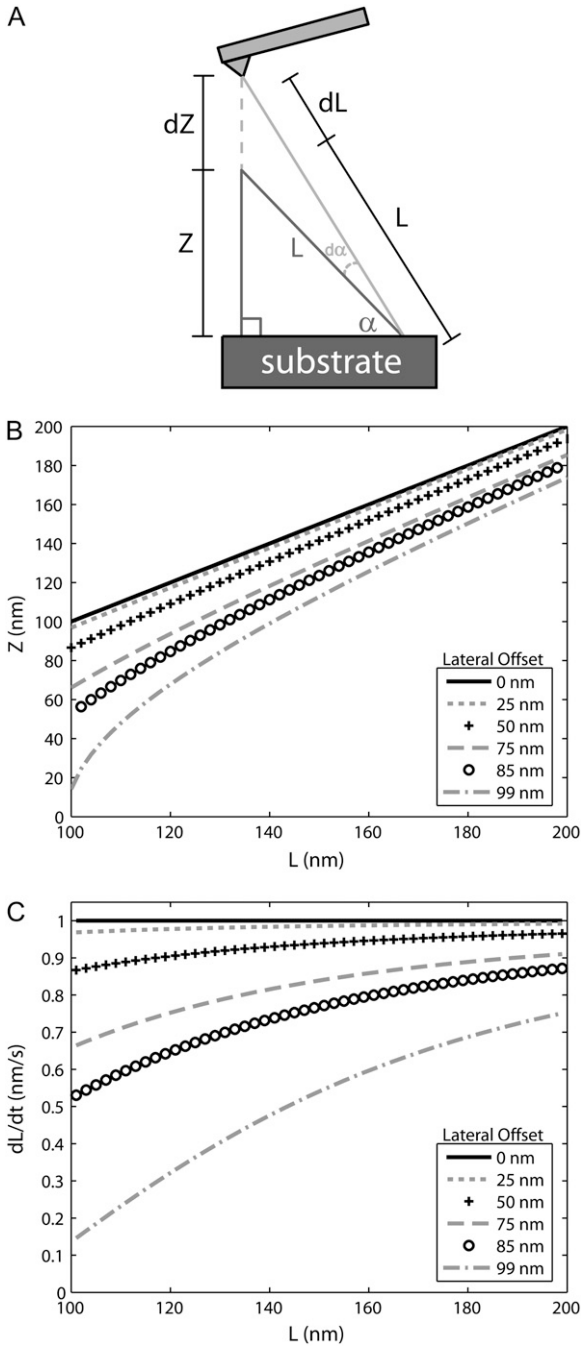

FIGURE 1 (*A*) AFM-SMFS pulling situation in which there is a lateral separation distance between the molecule's tip-sample attachment sites. (*B*) Measured (*Z*) versus actual length (*L*) for various lateral offsets. (*C*) Actual pulling velocity (*dL*/*dt*) for a vertical retraction rate (*dZ*/*dt*) of 1 nm/s. Lateral separation distance: 0 nm (*solid line*), 25 nm (*dotted shaded line*), 50 nm (*solid* +), 75 nm (*dashed shaded line*), 85 nm (○), and 99 nm (*dash-dot shaded line*).

the uneven loading caused by pulling geometry errors could further alter the shape and magnitude of the measured force-extension profile.

Depending on the length of the molecule and the lateral distance between the cantilever and substrate attachment sites, the impact on the recorded forces can be rather substantial. For instance, in our previous study (6), we've demonstrated that the lateral misalignments of DNA attachment sites were capable of altering the magnitude and length of measured B-DNA to S-DNA (BS)-transition plateaus by up to 62%. Because our understanding of molecules depends on the accurate representation of the force-extension profile, a method is needed to minimize the effects of pulling geometry errors during the data collection process. Although it is possible to determine the substrate attachment location of a molecule through repeated stretching and systematic adjustment of the *x*, *y* position of the cantilever, this method is extremely time consuming, and as a result, the likelihood of detaching the molecule during this process is extremely high. Alternative techniques have focused on minimizing torsional effects through the use of gimballed probes (10); however, this method relies entirely on custom cantilever probes. Because the availability and stiffness range of these cantilevers is limited, an alternative method to minimize pulling geometry effects is needed.

In this study, we investigated a software-based method to align a molecule's substrate and cantilever attachment sites before completely unraveling it with the AFM. Results from both simulation and experimental implementation of the alignment program are presented.

MATERIALS AND METHODS

AFM instrumentation

All experiments were carried out on our custom three-axis AFM. The AFM is equipped with a MultiMode AFM head from Digital Instruments (Veeco Metrology, Santa Barbara, CA) and two piezoelectric positioning stages from Physik Instrumente (Auburn, MA). The *x*, *y* stage (P-733.2CL) has a scanning range of 100 × 100 μm and a closed-loop resolution of <0.3 nm and the *z* stage (P-753.11C) has a traveling range of 12 μm and a resolution of 0.05 nm. The AFM head is mounted on the *x*, *y* stage, which is suspended above the *z* stage via three high-precision screws. Substrate samples are mounted onto the *z* stage such that the AFM head remains stationary during approach/retraction cycles. The control scheme for the AFM was designed in MATLAB's Simulink environment (The MathWorks, Natick, MA) and was digitally implemented through the use of a dSPACE (Wixom, MI) DAQ card (DS1104).

Alignment software

The alignment program, which is based on methods used to track fluorescent molecules (11–13), eye movement in laser eye surgery (14), and airborne missiles (15), uses small, continuous circular movements to locate the molecule's substrate attachment site and to reposition the cantilever such that errors due to pulling geometry can be minimized. For this particular application, a partially stretched molecule will be subjected to a circling motion in the *x*, *y* plane using the AFM's *x*, *y* stage. Because the force on the molecule is dependent on its extension, the measured force will fluctuate up and down as the distance between the molecule's attachment sites increases and decreases, respectively. By measuring the phase lag between the circling input and the force output, the angle between the molecule's cantilever and substrate attachment sites can be calculated. Once this angle is calculated, the *x*, *y* stage will move a distance (*dR*) along this angular path and the program will loop again. Because the circling motion is continuous, the *x*, *y* coordinates will be updated until the force stops fluctuating and a stall position is reached. To

ensure that the molecule remains partially stretched throughout the alignment procedure, the molecule is held at a constant, user-defined force. However, because standard implementation of the force controller would eliminate the circling-induced force fluctuations required for the alignment process, a notch filter was entered into the feedback loop. The addition of this filter into the feedback loop is necessary for the alignment process as it allows only the gradual changes in force, such as those caused by relaxation of the molecule as the tip is moved incrementally toward the substrate attachment site, to be compensated for by the controller.

Simulation

For the alignment simulations, the AFM control scheme was adapted by replacing the position and photodetector inputs with reproduced data. Specifically, we assumed position tracking errors of zero, and force readings from the photodiode were replaced with simulated molecular data. The simulated molecular data was obtained from experimental force-extension measurements on a single DNA duplex at various pulling locations (6). Two of these force-extension measurements can be found in Fig. 2. For each pulling location, the BS-transition force and slope of the initial force increase was calculated. The BS-transition force was used to determine the coordinates of the molecule's substrate attachment site and the slope of the initial force increase was used to generate the simulated force data. A detailed description of these procedures can be found in the Supplementary Material (Data S1). For this particular molecule, the location of the substrate attachment site was found to occur at the x, y coordinates (237 nm, 187 nm).

The alignment program was tested by choosing a random cantilever starting location and running the program until a stall position was reached or until the program failed. The initial separation distance between the cantilever and the designated substrate attachment sites ranged from 38.3 nm to 1.15 μm. Program failure occurred when tracking failed and the cantilever-substrate separation distance began to increase. Twenty different starting locations were tested in the simulated environment and the speed and accuracy of each experimental trial was determined. From this data, the average final separation distance, the average root mean-square (RMS) of the separation distance, and the average speed of the cantilever were determined. Because the same 20 starting locations were kept consistent among data sets, a direct comparison of the simulation parameters (circling diameter, step size, and noise input) could occur.

Sample preparation

Dextran conjugate ($\alpha-(1\rightarrow6)$-D-glucan with biotin) (D7142, Invitrogen, Carlsbad, CA) was dissolved in phosphate-buffered saline at a concentration of 0.005% (wt vol); 50 μl of solution was deposited onto glass coverslips for drying. Extensive rinsing was followed before measurement to get a layer of dextran molecules tightly adsorbed to the glass surface. MLCT-AUNM series probes (Veeco Probes, Camarillo, CA) were used for the pulling experiments. All experiments were conducted in aqueous media (filtered deionized water or phosphate-buffered saline) at room temperature.

Experimental alignment

To determine the magnitude and nature of circling-induced force fluctuations, a number of control experiments were conducted. In these experiments, vertical forces were measured as a cantilever was moved in a single circle cycle. A variety of circling frequencies (f), circling diameters (C_d), and starting angles (θ_0) were analyzed both in the absence and presence of a tethered molecule. For this work, a custom, automated pulling program was used to ''catch'' a single dextran molecule without fully unraveling it. This program will be discussed in a future publication.

To test the efficacy of the alignment program, the force-extension curves obtained before and after the program must be collected. Using the aforementioned method to catch a molecule, two force-extension curves were obtained at the original binding location. The molecule was then stretched to a region in the initial slope increase, after which a force control was enabled. Immediately after the force clamp was applied, the centering program was implemented. For the data shown, the alignment program had a circling frequency of 5 Hz, a circling diameter of 20 nm, and a step size of ~0.3 nm. Once the stall position was reached, force control was disabled and the molecule was returned to its relaxed state. Two additional force-extension curves were gathered at this location.

RESULTS AND DISCUSSION

Alignment simulations

The cantilever trajectories of a subset of the alignment trials superimposed on the contour plot of the experimental DNA BS-transition forces can be found in Fig. 3. Each of the alignment trajectories (*black lines*) makes a counterclockwise spiral toward the molecule's designated substrate attachment site (*green open circle*). Because the BS-transition forces decrease with increasing lateral separation distances (6), the contour plot of these forces serves as a visual cue to track the progress of the program during the alignment process. As

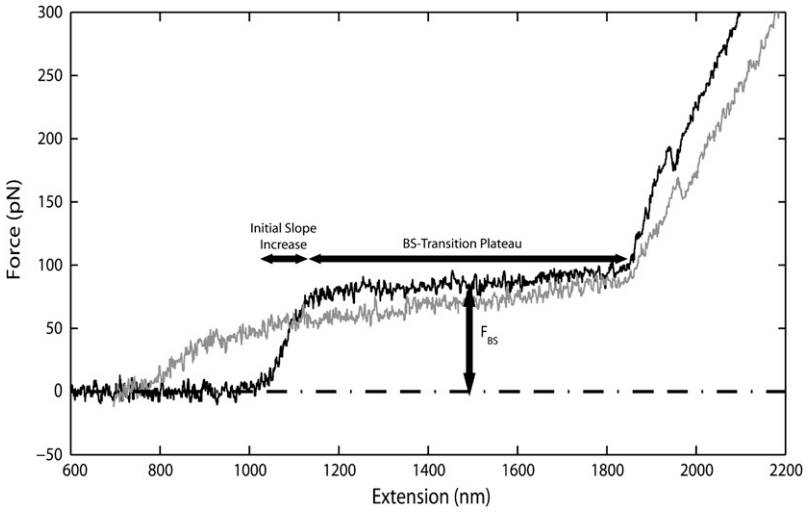

FIGURE 2 Experimental force versus extension plots of double-stranded λ-phage DNA obtained with an AFM at x, y positions (0 nm, 0 nm) (*solid trace*) and (0 nm, 800 nm) (*shaded trace*). The pulling positions are relative to the first pull (0 nm, 0 nm) and are given in nanometers. The initial force increase, the BS-transition plateau region, and the BS-transition force for pull (0 nm, 0 nm) are labeled.

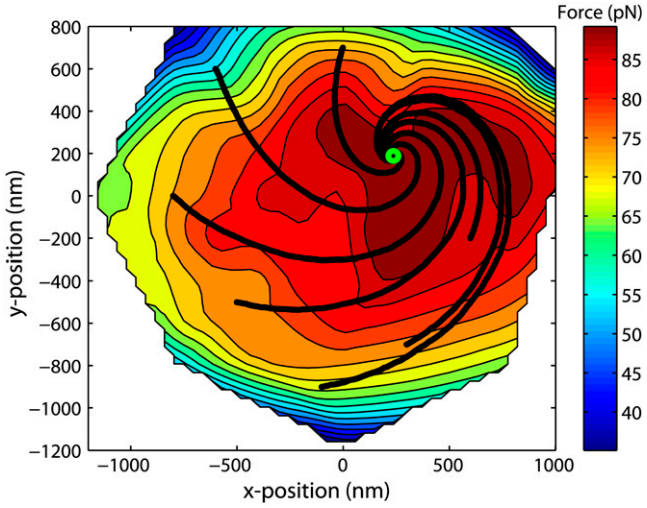

FIGURE 3 Trajectories taken by the cantilever during simulation (*black lines*) overlayed on the contour plot of the measured plateau forces. Each of the simulations shown here had a circling diameter of 30 nm, a step size of 0.8 nm, and an RMS noise input of 17 pN. The maximum BS-transition force occurs at position (237 nm, 188 nm) and is labeled with an open green circle.

the cantilever spirals in toward the substrate attachment site, the distance between the two molecular attachment sites decreases until the stall position is reached. The average distance between the final cantilever position and the substrate attachment site is 1.8 nm, a dramatic improvement from the initial separation distances (38.3 nm–1.15 μm).

Provided that the simulated stage trajectory remained within the confines of the modeled data (*colored region* in Fig. 3) and the circling diameter was large enough to create circling-induced force fluctuations that were larger than the noise in the force readings, the program was 100% successful in aligning the cantilever with the designated substrate attachment sites. For an RMS noise input of 17 pN, the circling diameter must be greater than or equal to 20 nm, as diameters of 10 nm had a 50% success rate and diameters of 5 nm had a 0% success rate. As can be seen from Table 1, increasing the circling diameter has little effect on the accuracy of the alignment program, as there was minimal improvement in the final separation distances (d_f) for trials 3–5. Increasing the circling diameter does, however, decrease the time needed to reposition the cantilever, as evidenced by the increase in cantilever velocity (V). This increase in velocity is the result of fewer missteps in the program. With larger circling diameters, it is easier for the program to identify the circling-induced force fluctuations in the force readings, and therefore the likelihood of calculating an incorrect phase lag is minimized. Therefore, for experimental implementation of the alignment program, the centering diameter should be maximized within the physical constraints of the molecule.

As can be seen in Table 2, decreasing the step size had the benefit of increasing the accuracy of the alignment, albeit at

TABLE 1 Simulation results for various circling diameters

Trial	C_d (nm)	% Success	Mean d_f (nm)	RMS d_f (nm)	V (nm/s)
1	5	0	—	—	—
2	10	50	2.25*	1.72*	2.93*
3	20	100	1.86	1.40	3.48
4	30	100	1.80	1.40	3.83
5	40	100	1.78	1.40	3.92

Desired force set point, 50 pN; circling frequency, 10 Hz; step size, 0.8 nm; and RMS of noise input, 17 pN.
*Averages calculated from successful data trails.

TABLE 2 Simulation results for various step sizes

Trial	dR (nm)	% Success	Mean d_f (nm)	RMS d_f (nm)	V (nm/s)
1	0.4	100	2.55	0.97	1.92
2	0.8	100	1.80	1.40	3.83
3	1.6	100	4.01	1.91	7.74
4	4.0	100	2.87	2.74	19.37
5	8.0	100	5.00	3.77	39.23

Desired force set point, 50 pN; circling frequency, 10 Hz; circling diameter, 30 nm; and RMS of noise input, 17 pN.

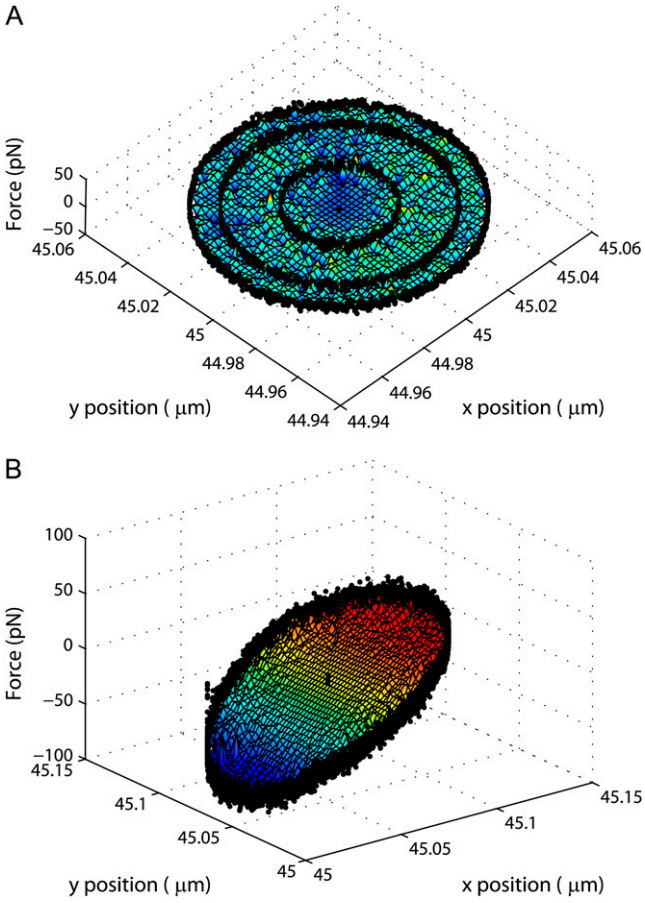

FIGURE 4 Surface plots generated from forces measured during circling. The measured forces from which the surface plots are generated are designated with black dots. (*A*) In the absence of molecular attachment (f = 1 Hz, C_d = 40, 80, and 100 nm). (*B*) In the presence of a molecular attachment (f =1 Hz, C_d = 100 nm).

the expense of velocity. The alignment program was designed such that the cantilever position is updated continuously by taking small steps toward the substrate attachment site. Due to noise in the force signal, there is a degree of error associated with calculating the phase lag. However, with continuous circling, the overall stage movement will be correct even if individual stage movements are incorrect. This continual updating of the cantilever position will drastically improve the accuracy of alignment. With predetermined step sizes, however, the cantilever will overstep the attachment site and oscillate around the substrate attachment site. With larger step sizes, the diameter of this oscillation increases, as evidenced by the RMS noise in the final separation distance (RMS d_f).

Control experiments

Before the alignment program was implemented, a number of control experiments to determine the magnitude and nature of circling-induced force fluctuations were conducted. In these experiments, vertical forces were measured as a cantilever was moved in a single circle cycle. A variety of circling frequencies, circling diameters, and starting angles were analyzed both in the absence and presence of a tethered molecule.

Fig. 4 *A* contains the surface plot of the forces during circling when no molecules were tethered between the cantilever and substrate. For all three diameters tested (40 nm, 80 nm, and 100 nm), the forces were constant throughout the circling cycle, ($F_{ave} = 0 \pm 5.2$ pN). The results shown are consistent for all experiments in which no molecular tether was present. Additional variables that were tested include sample position and circling frequency ($f = 0$–5 Hz), although this data is not shown. Although there is some variability in measured forces in these tests, the magnitude of these fluctuations are not believed to be large enough to significantly alter cantilever movement during the alignment process.

Fig. 4 *B* contains the surface plot of the forces during circling when a molecular attachment is present. The plot was generated from five individual circling cycles with a circling diameter of 100 nm and a frequency of 1 Hz. To demonstrate the positional dependency of the force, the circling cycles were started at five different positions along the circling path. The angles, θ_0, associated with these starting positions were

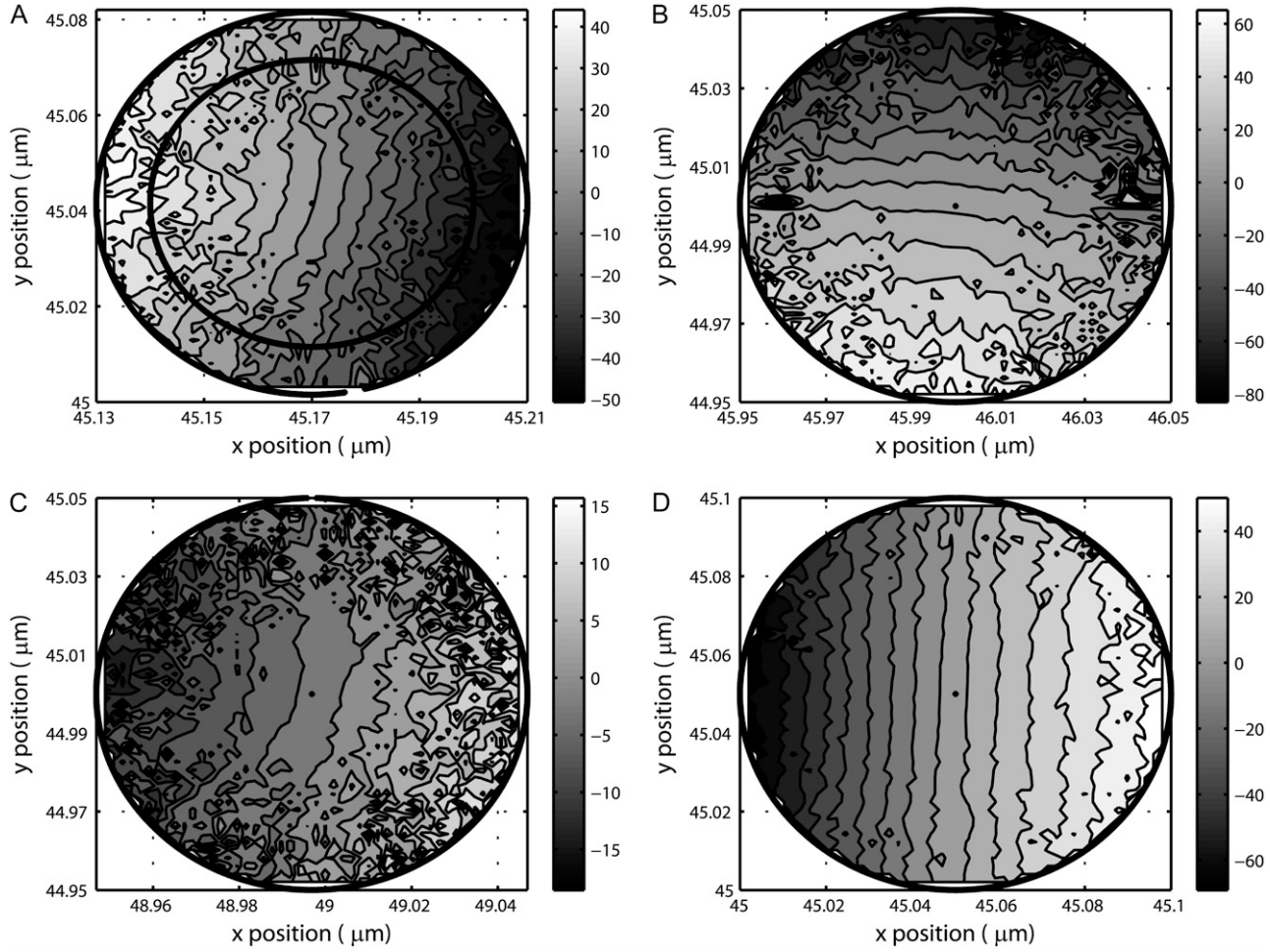

FIGURE 5 Contour plots of measured forces for four different molecular attachments. (*A*) $f = 1$ Hz, $C_d = 60$ nm, and 80 nm, $\theta_{min} = 342 \pm 7°$. (*B*) $f = 1$ and 5 Hz, $C_d = 100$ nm, and $\theta_{min} = 87 \pm 29°$. (*C*) $f = 0.5$, 1, 5 Hz, $C_d = 100$ nm, and $\theta_{min} = 173 \pm 13°$. (*D*) $f = 1$ Hz, $C_d = 100$ nm, and $\theta_{min} = 179 \pm 12°$.

48°, 160°, 92°, 263°, and 143°, respectively. As the figure demonstrates, the force gradient remained uniform regardless of the starting angle, with larger forces associated with stretching of the molecule and smaller forces associated with relaxing of the molecule. The magnitude and location of the force minimum were consistent for all circling cycles, with an average value of -78 ± 4 pN at an angular location, θ_{min}, of $179 \pm 12°$. To investigate the effects of cantilever twisting on the measurements, the vertical forces 90° from the alignment axis of the surface fit were also calculated. These forces were -7 pN at 96° and 13 pN at 276°. Considering the instrumentation noise and the imprecise manner in which the alignment axis was determined, this difference is believed to be negligible. As a result, the symmetry of the forces about this alignment axis indicates that the effects of cantilever twisting on force measurements were negligible for this offset orientation.

Fig. 5 contains the force contour plots for four different dextran molecule attachments. As one can see, the alignment of the force gradient varies for each individual molecule, with the force minimums located at 342°, 87°, 173° and 179°. The variability in the alignment of the force gradients indicates that the measured force fluctuations are not artifacts from the piezoelectric stage movement or from the substrate sample slope. In addition, the variability in the magnitude of the forces indicates that the force fluctuations are indeed molecule specific.

Combined, these control experiments demonstrate that circling-induced force fluctuations are detectable with our instrumentation and verify that the source of the force fluctuations stems from changes in the extension of a tethered molecule.

Alignment experiments

Fig. 6 shows the trajectory taken by the cantilever during the alignment process. For this particular trial, the distance between the original binding location and the program's stall position was 58 nm. To keep the molecule partially stretched, the force controller continuously adjusted the position of the z stage such that the vertical distance between the sample and the substrate increased by a total of 7 nm over the course of the alignment.

Fig. 7 *A* contains the force extension profiles of the same dextran molecule obtained before (*shaded trace*) and after (*solid trace*) the alignment program was enabled. At the conformational transition, the measured forces of the after trace were substantially larger than that obtained at the original binding location. To verify that the force increase was due to alignment of the molecular attachment sites and not due to measurement noise or hysteresis, two consecutive pulls were obtained both before and after the alignment program was implemented and each set of curves was then averaged and analyzed. Fig. 7 *B* contains the information gathered from this analysis. At low extensions ($E < 85$ nm), the force difference between the before and after curves was comparable to the measurement noise for consecutive pulls. At higher extensions

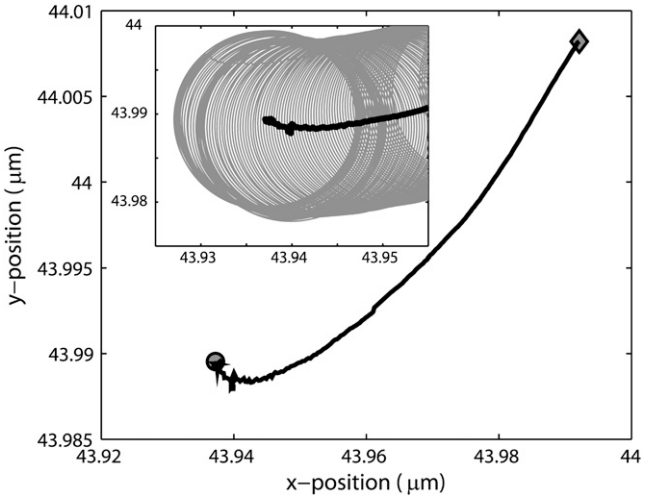

FIGURE 6 Path taken by the cantilever during the alignment process (*solid trace*). The original binding location is designated with a diamond and the stall position of the alignment program is designated with a circle. (*Inset*) Enlarged picture of the stall position with corresponding alignment trajectory (*solid trace*) and actual x, y stage motion (*shaded trace*).

($E > 85$ nm), however, the forces associated with the ''aligned'' molecule are substantially larger than that seen originally, with an average force increase of 129 pN during the conformational transition (85 nm $< E <$ 105 nm). In this key transitional region, the force increase (*solid region*) is more than twice the standard deviation of both the before and after traces combined (*shaded region*). Because the force extension curves were obtained on the same molecule, this suggests that repositioning the cantilever led to the force increase. By aligning the applied force with the measurement axis, the dextran molecule is no longer undergoing combined loading, and the full force was measured by the cantilever.

Due to the small step size (0.3 nm) and slow circling frequency (5 Hz), the alignment program took ~80 s to reach the stall position. Although this may seem long compared to the typical AFM-SMFS pulling time, one must consider the errors associated with such pulling techniques. Had the molecule in the case presented above not been aligned, the conformational transition force would have been underestimated by ~15%. Although it is rare that individual force-extension curves are analyzed, errors such as these will lead to a broadening of any resulting force histogram peaks and, as a result, will impact the accuracy of the subsequent data analysis. In a more general sense, it is possible that the surface chemistry-dependent binding strengths reported in the literature (3) may be related to pulling geometry effects that stem from chemistry-specific molecular orientation differences. Although the prevalence and impact of pulling geometry errors are not yet fully understood, if the sensitivity of AFM-SMFS studies is to improve, one must consider sacrificing speed for accuracy.

It is important to note that the aforementioned alignment time is a conservative value. For the proof-of-concept test shown here, the step-size and circling frequency was inten-

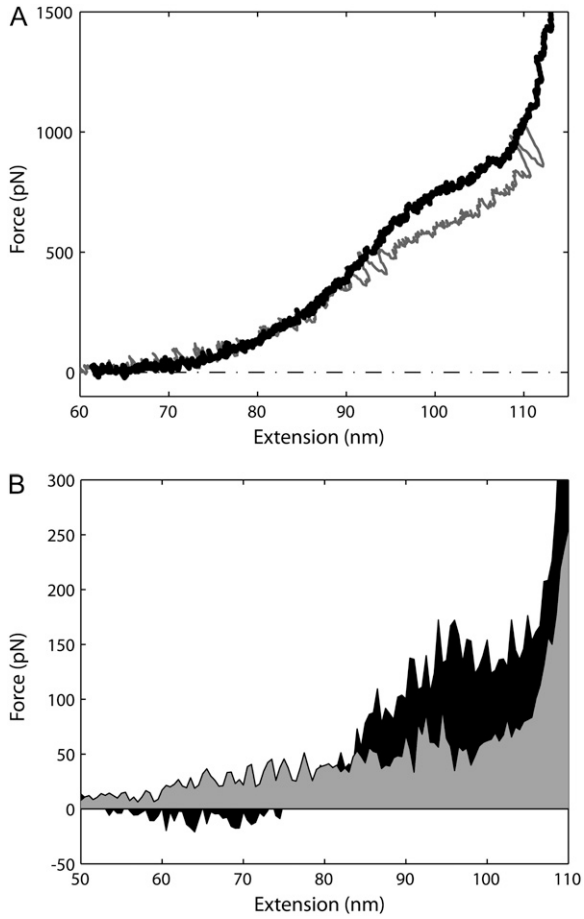

FIGURE 7 (*A*) Force-extension profile of a dextran molecule obtained at the original cantilever binding coordinates (*shaded trace*) and at the ''stall'' location of the alignment program (*solid trace*). The extension of the stall curve was increased by 10 nm to allow for easier comparison between the measured conformational transition forces. (*B*) Averages of two consecutive pulls both before and after the alignment program was implemented were used to calculate the force increase (*solid region*) associated with repositioning the cantilever. The shaded region depicts the combined standard deviation associated with the before and after alignment averages.

tionally chosen to be small to minimize the likelihood of unbinding during the alignment process. As per the simulation data, it is possible to decrease the alignment time by increasing these values accordingly. Even at its current speed, the alignment program is much faster than manual alignment techniques. In a parallel study on a single dextran molecule, manual alignment of the molecule required >100 force-extension curves that were recorded over ~1 h. A subset of these curves can be found in Fig. 8.

CONCLUSIONS

In this article, we have demonstrated the ability of a custom software-based method to decrease pulling geometry errors in AFM-SMFS. Whereas other researchers have focused on minimizing pulling geometry errors through the use of analytical techniques (5,7) or custom, dual-axis gimballed probes

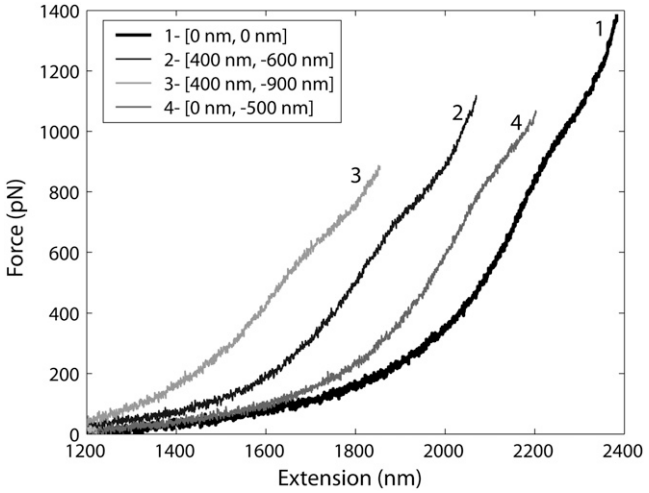

FIGURE 8 Subset of the experimental force versus extension plots of dextran obtained during manual alignment. The traces are numbered sequentially according to the chronological order in which they were obtained. The *x*, *y* coordinates for each trace can be found in the figure legend.

(10), this technique has the advantage of being able to be used experimentally with standard, commercially available cantilevers. Simulations on DNA have shown that the alignment program is capable of repositioning the cantilever to within 5 nm of the molecule's sample binding site. Single circle experiments conducted with and without a bound molecule suggest that circling-induced fluid fluctuations are not a hindering factor in the detection process for the frequencies tested. Furthermore, the variability in the alignment axis of the molecules indicates that the circling-induced force fluctuations are molecule specific and not caused by artifacts from the stage movements. The force-extension curves obtained before and after full implementation of the program suggest that aligning the applied force with the measurement axis dramatically alters the magnitude of the forces measured by AFM. For the case presented, the force increase associated with the alignment process was ~129 pN at the conformational transition of dextran. Although the alignment results are positive, it is important to stress that the aforementioned alignment program can only minimize pulling geometry errors and not boundary deflection errors associated with the molecular attachment geometry (5,7). However, because pulling geometry errors have been shown to dramatically alter the forces and extensions measured with the AFM, we believe that the alignment program presented herein will become a valuable tool for improving the accuracy of AFM-SMFS studies.

SUPPLEMENTARY MATERIAL

To view all of the supplemental files associated with this article, visit www.biophysj.org.

This work was funded by grants from the National Science Foundation and National Institutes of Health to P.E.M. and R.L.C.

REFERENCES

1. Binnig, G., C. F. Quate, and C. Gerber. 1986. Atomic Force Microscope. *Phys. Rev. Lett.* 56:930–933.
2. Rief, M., and H. Grubmuller. 2002. Force spectroscopy of single biomolecules. *ChemPhysChem.* 3:255–261.
3. Janshoff, A., M. Neitzert, Y. Oberdorfer, and H. Fuchs. 2000. Force spectroscopy of molecular systems single molecule spectroscopy of polymers and biomolecules. *Angew. Chem. Int. Ed.* 39:3213–3237.
4. Zlatanova, J., S. M. Lindsay, and S. H. Leuba. 2000. Single molecule force spectroscopy in biology using the atomic force microscope. *Prog. Biophys. Mol. Biol.* 74:37–61.
5. Kulic, I. M., H. Mohrbach, V. Lobaskin, R. Thaokar, and H. Schiessel. 2005. Apparent persistence length renormalization of bent DNA. *Phys. Rev. E.* 72:041905.
6. Ke, C., Y. Jiang, M. Rivera, R. Clark, and P. E. Marszalek. 2007. Pulling geometry induced errors in single molecule force spectroscopy measurements. *Biophys. J.* 92:L76–L78.
7. Hori, Y., A. Prasad, and J. Kondev. 2007. Stretching short biopolymers by fields and forces. *Phys. Rev. E.* 75:041904.
8. Evans, E., and K. Ritchie. 1997. Dynamic strength of molecular adhesion bonds. *Biophys. J.* 72:1541–1555.
9. Rief, M., M. Gautel, F. Oesterhelt, J. M. Fernandez, and H. E. Gaub. 1997. Reversible unfolding of individual titin immunoglobulin domains by AFM. *Science.* 276:1109–1112.
10. Beyder, A., and F. Sachs. 2006. Microfabricated torsion levers optimized for low force and high-frequency operation in fluids. *Ultramicroscopy.* 106:838–846.
11. Berglund, A. J., and H. Mabuchi. 2004. Feedback controller design for tracking a single fluorescent molecule. *Appl. Phys. B.* 78:653–659.
12. Enderlein, J. 2000. Tracking of fluorescent molecules diffusing within membranes. *Appl. Phys. B.* 71:773–777.
13. Kis-Petikova, K., and E. Gratton. 2004. Distance measurement by circular scanning of the excitation beam in the two-photon microscope. *Microsc. Res. Tech.* 63:34–49.
14. Naess, E., T. Molvik, D. Ludwig, S. Barrett, S. Legowski, C. Wright, and P. de Graaf. 2002. Computer-assisted laser photocoagulation of the retina—hybrid tracking approach. *J. Biomed. Opt.* 7:179–189.
15. Esker, A., J. L. Manche, and R. M. Siler. 1977. Missile Director. United States Patent No. 4,014,482, March 29, 1977.